ChemPubSoc Europe

DOI: 10.1002/cphc.201301080

Cryogenic Colocalization Microscopy for Nanometer-Distance Measurements

Siegfried Weisenburger,*[a] Bo Jing,[b, c] Dominik Hänni,[d] Luc Reymond,[d, e] Benjamin Schuler,[d] Alois Renn,[b] and Vahid Sandoghdar*[a]

The main limiting factor in spatial resolution of localization microscopy is the number of detected photons. Recently we showed that cryogenic measurements improve the photostability of fluorophores, giving access to Angstrom precision in localization of single molecules. Here, we extend this method to colocalize two fluorophores attached to well-defined positions of a double-stranded DNA. By measuring the separations of the fluorophore pairs prepared at different design positions, we verify the feasibility of cryogenic distance measurement with sub-nanometer accuracy. We discuss the important challenges of our method as well as its potential for further improvement and various applications.

1. Introduction

The rise of super-resolution microscopy during the past decade has advanced fluorescence far-field microscopy beyond the diffraction limit.[1,2] One prominent method relies on localizing the position of single fluorescent molecules, whereby the center of the imaged point-spread function (PSF) of each molecule is determined with a much higher precision than its width. The central idea of this strategy dates back to as early as the 1920s by Werner Heisenberg[3] and was implemented experimentally to find the position of a nanoscale object with nanometer precision at the end of the 1980s.[4] In this approach, individual molecules can be localized with arbitrary precision if only sufficiently high signal-to-noise ratio (SNR) is available.

To distinguish or "resolve" close-lying points, localization microscopy methods implement various schemes to record the fluorescence of the molecules in the sample one after the other, so that the position of each individual molecule can be determined independently.[5] The localization precision for single molecules translates then directly to the resolving capability of the technique. Indeed, colocalization of single molecules was demonstrated in the early 1990s by selective excitation of narrow transitions within the inhomogeneous distribution of molecular resonance frequencies at liquid helium temperature[6,7] soon after it became possible to detect single molecules.[8,9] In 2002, cryogenic high-resolution single-molecule spectroscopy was used to demonstrate nearly molecular resolution in all three spatial dimensions by creating position-dependent frequency shifts through the application of electric field gradients.[10] Extension of this spectral selectivity to room temperature has also been explored using multicolor nanocrystal quantum dots[11] or fluorescent molecules[12] but it is hampered by the broad overlapping emission spectra and chromatic aberration in the optics.

During the last decade, room-temperature localization microscopy techniques have been introduced based on the stochastic activation of fluorophores.[13–15] Here, the localization precision depends on the detected number of photons (N), the half-width (s) of the PSF given by the standard deviation of a Gaussian profile, the level of background noise (b) and the pixel size (a). The attainable localization precision (σ_{loc}) using a maximum-likelihood estimation procedure with a 2D Gaussian function can be written as [Eq. (1)]:

$$\sigma_{loc} = \sqrt{\frac{s^2 + a^2/12}{N}\left(\frac{16}{9} + \frac{8\pi(s^2 + a^2/12)b^2}{Na^2}\right)} \quad (1)$$

which predicts a localization error close to the information limit.[16] The limiting factor is typically the finite value of N caused by irreversible photobleaching of the fluorophore. The photon budget of commonly used photoactivatable fluores-

[a] S. Weisenburger, Prof. V. Sandoghdar
Max Planck Institute for the Science of Light
and Department of Physics
University of Erlangen-Nuremberg
91058 Erlangen (Germany)

[b] B. Jing, Dr. A. Renn
Laboratory of Physical Chemistry
ETH Zurich, 8093 Zurich (Switzerland)

[c] B. Jing
Current Address:
Biological Physics Research Group
Department of Physics, Clarendon Laboratory
University of Oxford, Parks Road
Oxford OX1 3PU (UK)

[d] Dr. D. Hänni, Dr. L. Reymond, Prof. B. Schuler
Department of Biochemistry
University of Zurich
8057 Zurich (Switzerland)

[e] Dr. L. Reymond
Current Address:
Institute of Chemical Sciences and Engineering (ISIC)
Ecole Polytechnique Fédérale de Lausanne (EPFL)
1015 Lausanne (Switzerland)

 © 2014 Wiley-VCH Verlag GmbH & Co. KGaA, Weinheim

cent proteins, for instance, lies in the range of a few hundred detected photons,[17] leading to a localization precision of about 20 nm. To improve on this, several efforts have optimized the choices of the fluorophore and the buffer condition,[18,12] engineered the dye molecule itself[19] or controlled its environment.[20] We have recently demonstrated that the significantly reduced rate of photochemistry at cryogenic temperatures allows single-molecule localization at Angstrom precision.[21] In this Article, we extend this exquisite precision to determine the separation of two neighboring fluorophores on the backbone of a double-stranded DNA as a model system. Furthermore, we discuss the systematic localization error that may arise due to the fixed orientation of the dipole emitter near an interface.

2. Results

Figure 1a shows the photostability improvement of single Alexa Fluor 532 molecules at 4 K in comparison to the performance of the same species at room temperature and under equivalent illumination conditions.[21] To colocalize two or several molecules within a diffraction-limited spot, it is necessary to detect the individual emitters sequentially. Because the absorption spectra of common dye molecules do not reduce beyond the inhomogeneous broadening of the spectrum, spectral selection via high-resolution spectroscopy is not possible in these systems.[8,9] An interesting alternative is to analyze the PSF corresponding to discrete intensity levels of stepwise bleaching or blinking of single molecules.[22–25] In this work, we follow the latter strategy.

First, we extract a fluorescence intensity trace for a single PSF from an image stack recorded at a frame rate of about 5 Hz. This frame rate turned out to be a good compromise between a reasonable time resolution to capture fast blinking events and a SNR of $\approx$50 per frame, which is high enough for reliable localization. Figures 1b and 1d plot two different examples of blinking traces, showing discrete levels of intensity, corresponding to both or one of the molecules fluorescing. We then identify the intensity levels (solid lines in Figure 1b) using a total variation-based denoising[26] and plot histograms of the fluorescence intensities as displayed in Figures 1c and 1e for the traces of Figures 1b and 1d, respectively. Once we have identified the blinking intervals, we sum the frames within each one to improve the SNR. We then determine the position $\vec{x}_1$ of one of the molecules from the PSF of a low-intensity interval. An example of the diffraction-limited spot corresponding to the interval marked by an arrow in Figure 1b is displayed in Figure 2a. Figure 2b shows a line cut from this PSF as well as a fit that yields a localization precision of 7 Angstroms (corresponding to a SNR of $\approx$3000). Next, we find the PSF center of mass $\vec{x}_c$ of the fluorophore pair from one of the neighboring high-intensity intervals and compute the distance between the two molecules by accounting for the fluorescence intensities of the two molecules in a weighted fashion. The position $\vec{x}_2$ of the second molecule is then computed as [Eq. (2)]:

$$\vec{x}_2 = \frac{N_c\vec{x}_c - N_1\vec{x}_1}{N_c - N_1} \quad (2)$$

where N_1 and N_c denote the number of photons of the first molecule and the center of mass spot, respectively.

As shown by several examples in Figures 2c–e for different DNA constructs, we plot the extracted distance values from various interval pairs of each blinking trace in a histogram and perform a maximum likelihood estimation with the Rician distribution to obtain mean and accuracy values. The results are displayed by the fits in Figures 2c–e. The two localized positions are normally distributed in space with a certain localization precision. The distribution of the distance between both positions is not Gaussian but the Euclidian norm of a bivariate normal distribution called a Rician distribution.[27] Importantly, the expectation value of this asymmetric distribution does not coincide with the peak position so that a Gaussian fit would introduce a systematic error towards a larger distance. All stated localization precision values were computed from the covariance matrix of the fitting procedure by error propagation of the variance of the residuals. Individual frames where the localization precision was worse than the design distance, for example, for very short blinking intervals, were discarded. We note that the variations in the number of distance readings in the examples of the histogram stem from the different characters of the observed blinking behavior, for example, shown in Figures 1b,d.

Figure 3a sketches the example of a DNA construct with a nominal distance of 10 nm, for which we find a distance of 11.8 nm $\pm$ 1.2 nm between the two fluorophores. Figure 3b shows the results for DNA constructs of four different design fluorophore separations of 10 nm (30 base pairs, bp), 6.7 nm (20 bp), 5.0 nm (14 bp), and 3.3 nm (10 bp). The open circles in Figure 3b denote individual measurements and the error bars show the standard error of the mean. The data clearly confirm the ability of cryogenic colocalization to read the distances of single molecules in the range well below ten nanometers. We mention in passing that one has to keep in mind that the size of an Alexa Fluor 532 molecule itself (molecular weight of 720 Da) is approximately 1.3 nm and it is attached to the nucleoside via a linker of six methylene groups. This uncertainty in position due to label and linker size is averaged out due to symmetry when looking at multiple DNA molecules.

3. Discussion

We now discuss a few intriguing features of the physics and open questions involved in our experiments as well as an analysis of the localization precision and accuracy. Curiously, the fraction of DNA molecules that showed more than one discrete intensity level in their blinking trace was much lower than expected. For instance, in the case of the DNA constructs with 10 nm separation we recorded about 12000 traces from wide-field image stacks. Only less than 10% of these showed two distinct levels of fluorescence intensity. We emphasize that in room-temperature experiments we verified that this low yield was not caused by suboptimal labeling. After excluding the

© 2014 Wiley-VCH Verlag GmbH & Co. KGaA, Weinheim

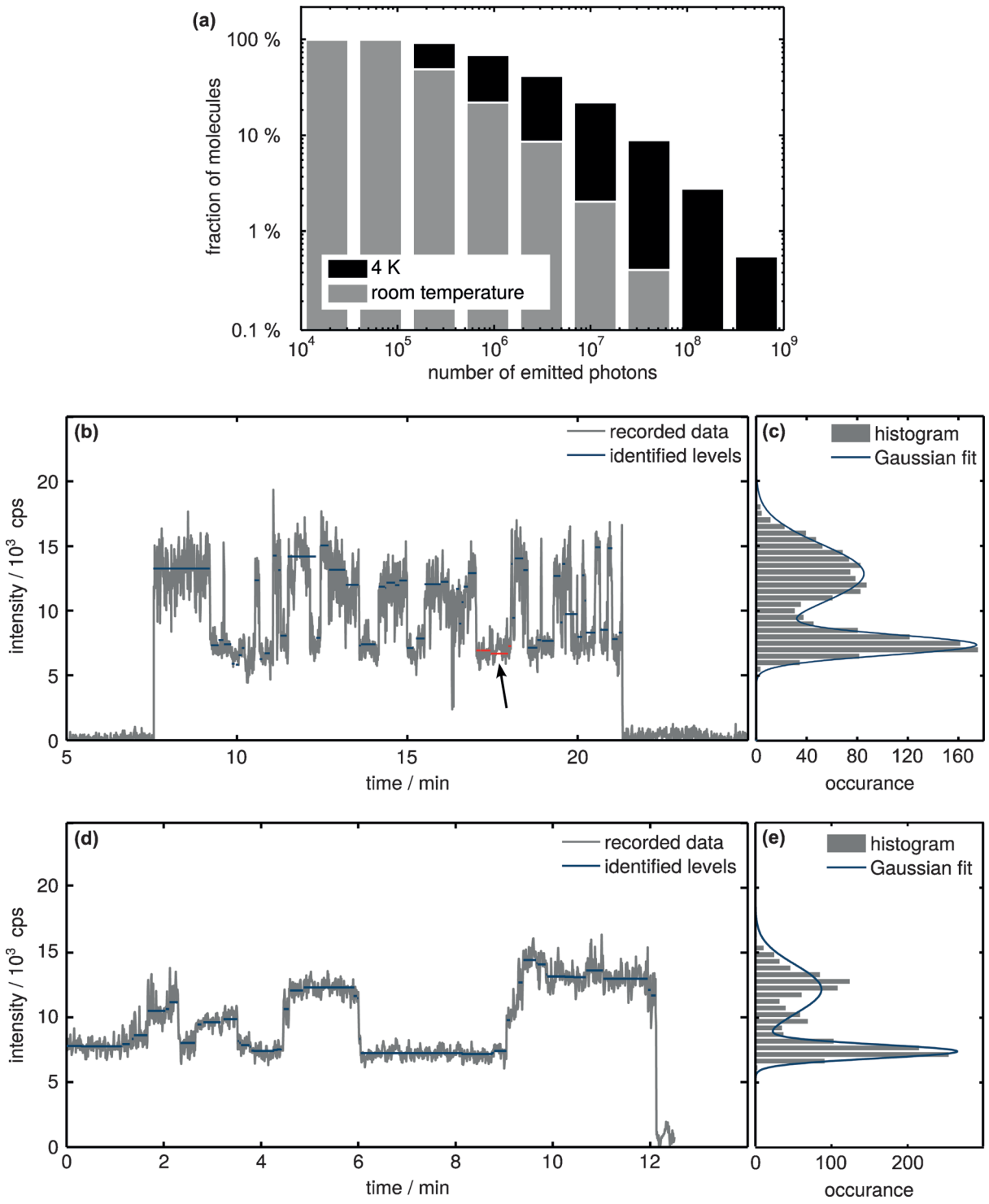

Figure 1. Photostability at low temperature and blinking behavior. a) Cumulative histograms of the total number of emitted photons for single Alexa Fluor 532 molecules at low temperature and at room temperature under equivalent illumination conditions. b) An example of a fluorescence trace of a single DNA construct labeled with two Alexa molecules. The arrow marks the interval (red) for which the PSF is shown in Figure 2a,b. c) Histogram of the fluorescence intensities (gray) and a double Gaussian fit (blue). d, e) Same as (b,c) but for a different DNA construct.

traces, where either two separate fluorophores accidentally lay close by (i.e. the extracted distance was well above the design value) or the SNR was too low, about 0.1% of the original traces could be used for colocalization. For DNA constructs with smaller fluorophore separation this fraction was even lower. A second noteworthy finding is that we never observed total off-states (i.e. both fluorophores off) in the blinking traces. Assuming a scenario where the off-state is caused by a photo-induced charge separation and subsequent charge trapping in the vicinity of the fluorescent molecule,[28] a low

© 2014 Wiley-VCH Verlag GmbH & Co. KGaA, Weinheim

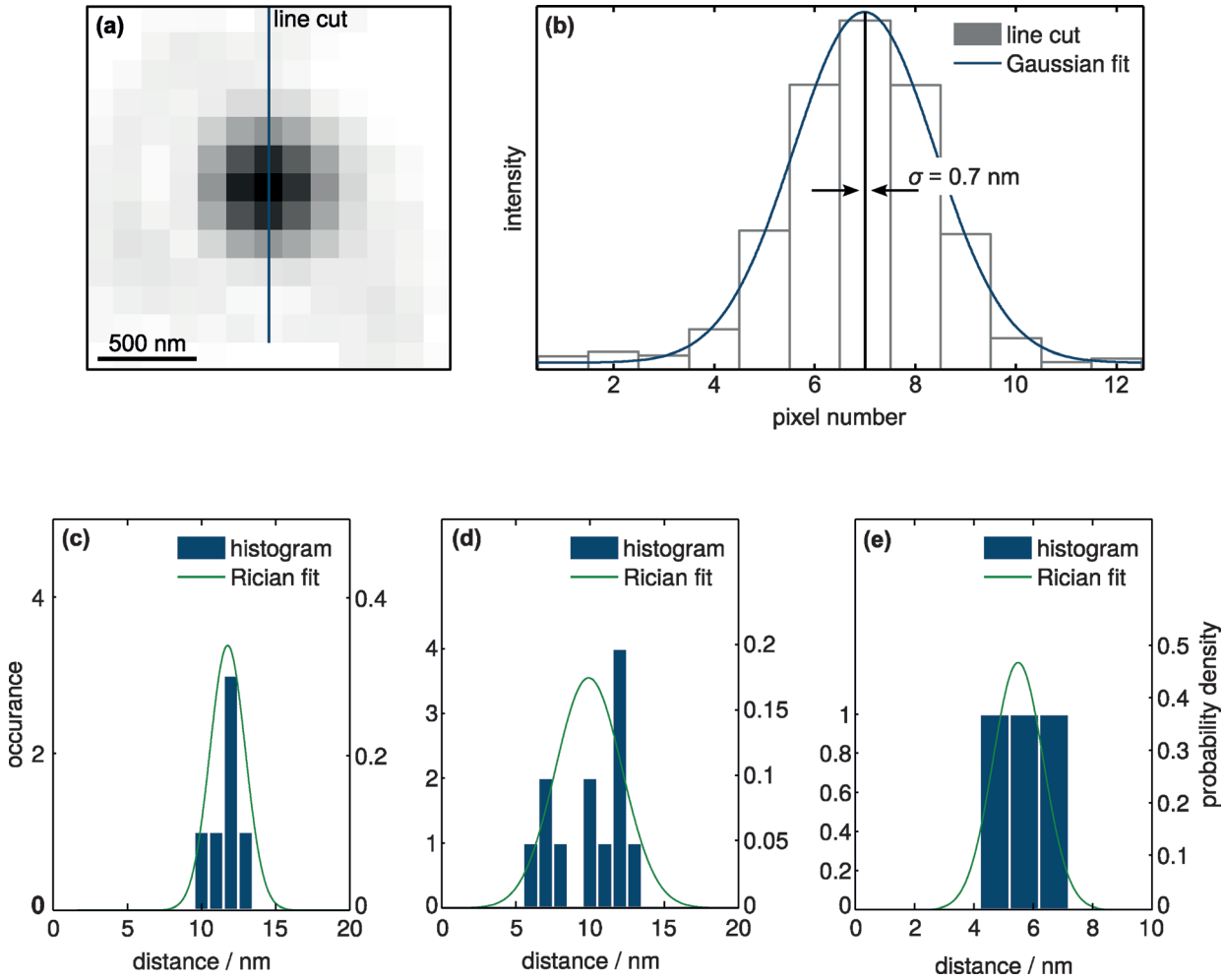

Figure 2. Colocalization analysis. a) Diffraction-limited spot on the camera chip from the interval marked in Figure 1 b. b) Line cut (gray) and Gaussian fit (blue). The black line illustrates the position of the center determined with a precision of 0.7 nm. c–e) Three examples of histograms of the distances determined from individual steps between adjacent intervals of the blinking traces (blue). The green curves show fits according to a Rician distribution to determine the mean distance and the accuracy of the distance measurements.

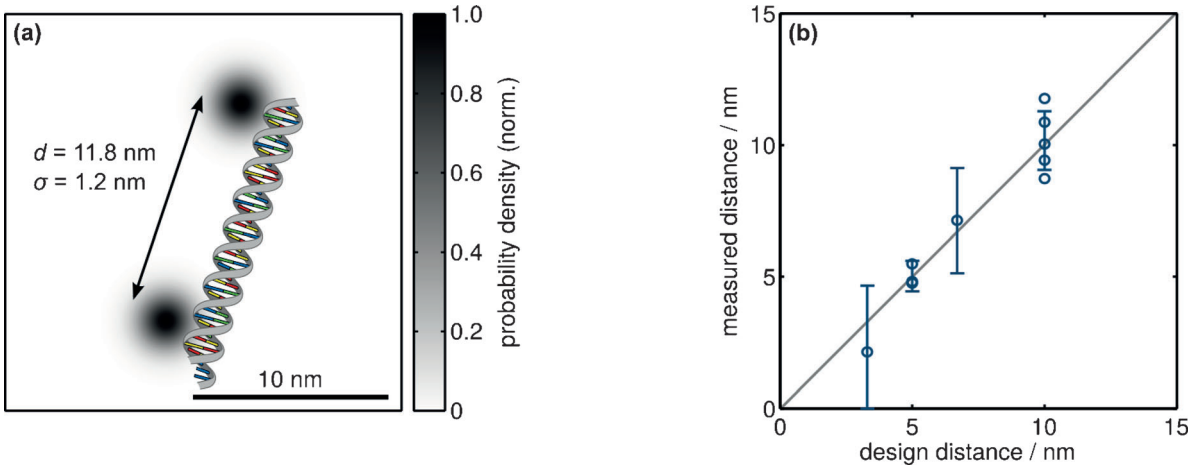

Figure 3. Cryogenic colocalization measurements. a) Visualization of the mean positions and localization precision for a DNA construct with two Alexa Fluor 532 labels placed at a separation of 10 nm. b) Results of DNA constructs with four different fluorophore design distances of 10 nm (30 base pairs, bp), 6.7 nm (20 bp), 5.0 nm (14 bp), and 3.3 nm (10 bp). Each open circle denotes a measurement of one fluorophore pair. Error bars show the standard error of the mean.

© 2014 Wiley-VCH Verlag GmbH & Co. KGaA, Weinheim

number of possible trapping sites or a filled trap could explain this observation. Furthermore, the distribution of intensities for the higher level was always broader than that of the lower level by 2–3 times. While a factor of $\sqrt{2}$ can be attributed to a larger shot noise, we do not have a robust explanation for this discrepancy. Another interesting observation is that blinking off and on states last for tens to hundreds of seconds, whereas the same samples display much faster blinking at room temperature. These long residence times facilitate the high localization precisions reported in this work. Finally, we did not encounter two-step bleaching events. In other words, no recorded trace showed a transition from two active fluorophores to a state, where only one fluorophore was alive for a long time.

The photophysics and photochemistry of nearby molecules can be complex. Various phenomena such as dipole–dipole coupling and fluorescence energy transfer[29–31] as well as nontrivial distribution of charges and chemically-active elements such as oxygen might be at play. A proper understanding of these processes requires extensive spectroscopic studies which are beyond the scope of this report. Our goal here has been to present the first results of cryogenic localization microscopy and demonstrate its promise for ultraprecise measurement of distances, for example, for determining the separations of protein domains. The data in Figure 3b indicate that reliable information can be extracted even from a small number of runs although more measurements would also clearly reduce the measurement uncertainty.

The success in single-molecule localization critically depends on both the precision and accuracy of the employed method. The precision is usually defined as the standard deviation of the estimated positions, while the accuracy quantifies how close the estimated position lies to the true position. The localization precision is mainly determined by the spot size and the number of photons that can be collected from the emitter before it photobleaches. Other factors besides pixelation are mostly due to the background,[32,33] which might be caused by luminescence from the cover glass or other elements in the optical path as well as the camera dark counts and read-out noise.[34] One of the origins of the limited accuracy is the nonuniformity in the camera pixel response (PRNU).[12] In our experiment, the camera has a PRNU standard deviation of about 0.5%. We verified in simulations that this causes a maximal systematic deviation from the true position of less than 0.5 nm. Furthermore, since both emitters are very close and see the same PRNU landscape on the camera, this factor is negligible for our measurements. Another effect that could affect the localization accuracy is the overlapping PSFs of neighboring entities. This systematic error starts to be insignificant for inter-PSF distances of about six pixels or more in our configuration. Thus, we avoided samples with too high fluorophore densities and excluded those data when there was another spot too close.

The strongest systematic localization error is by far due to the emission characteristics of a fixed dipole of arbitrary orientation at an interface. It is generally known that dipole emitters with an inclination angle outside the horizontal plane produce asymmetric PSFs. As a result, a localization method based on a centroid calculation or a 2D Gaussian fit cannot determine the actual position of the dipole emitter.[35,36] Even in the case of rotating dipoles a systematic position error remains when the molecular rotation is partially impaired.[37,38] It has been pointed out that this asymmetry and its associated localization error are much less pronounced if a microscope objective with low numerical aperture is used.[36] Another source of error that has been identified concerns defocusing.[37,39]

To investigate these effects theoretically, we calculated artificial PSFs numerically using the Kirchhoff vector approximation following the work of Mortensen et al.[16] and references therein. The calculations were performed for an emission wavelength of 555 nm and a simple generic geometry with one interface between two media of refractive indices $n=1.0$ and $n=1.5$ (see Figure 4a). In Figure 4b, we show some examples of calculated PSFs for two different numerical apertures (NA) of the collection optics and different polar angles (Θ) of the dipole orientation. It is evident that the degree of asymmetry is much less for NA = 0.75 as compared to the case of high NA. By fitting these detected patterns with the conventional procedure, we compared the true and "measured" positions of the dipole. Figure 4c displays the results of the calculated localization error as a function of NA and Θ, where the dipole was placed close to the interface (distance $z=2$ nm) inside the low-index medium, and detection took place through the high-index material assuming an index-matched immersion situation. We find that the systematic localization error is negligible (less than a few Angstroms) if the imaging optics only collects the emission below the critical angle (i.e. NA <1). However, it can increase to about 13 nm for high NAs and certain dipole orientations. When the detection is through the low-index medium (not shown), we find that the systematic localization error is comparable to the case shown in Figure 4c for NA $<$ 1 and is also negligible. In addition, we examined the influence of the dipole–interface distance z, while the dipole was kept in the focal plane at all times (again detecting through the high-index medium). Figure 4d shows the result for NA = 0.75, revealing that for increasing z, the maximal systematic localization error increases and reaches about 6 nm at $z=100$ nm.

In the experiments reported here, the DNA strands carrying the fluorophores lay at the interface so that the effective separation of the center of mass of the dipoles and the interface was of the order of one nanometer. Furthermore, we could only use a microscope objective with a low numerical aperture of NA = 0.75. As a result, dipole emitters with out-of-plane orientation were less efficiently excited, and large-angle components of the emission were not captured. It turns out, therefore, that the localization accuracy of our measurements is not compromised in this arrangement.

4. Outlook

Recently, we reported Angstrom precision in single-molecule localization at cryogenic temperatures.[21] In this work, we have extended those results to colocalization of two identical fluorescent molecules placed at nanometer distances. The aim of

© 2014 Wiley-VCH Verlag GmbH & Co. KGaA, Weinheim

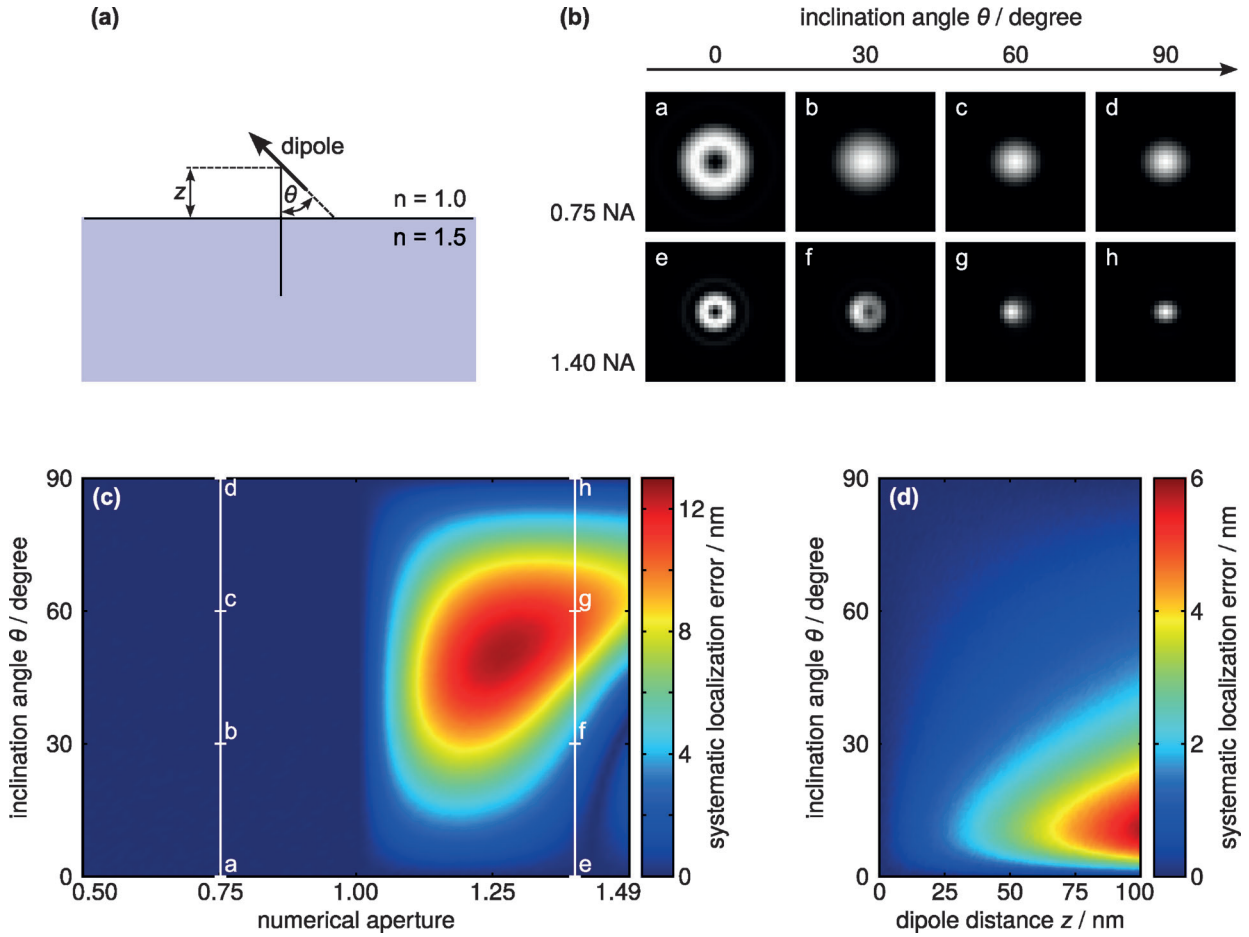

Figure 4. Systematic localization error for fixed dipoles fitted with a 2D Gaussian. a) Geometry for the simulations. The molecules have a polar angle Θ and a distance to the interface between the two media z. b) Examples of calculated PSFs for two different numerical apertures and four polar angles. c) Simulation of the error in the localization accuracy for varying numerical aperture and polar angles Θ, assuming $z = 2$ nm. d) Simulation of the error in the localization accuracy as a function of z and Θ, assuming NA = 0.75.

this work has been to demonstrate the feasibility of cryogenic colocalization for measuring separations of molecules in the range well below ten nanometers. This method is particularly promising for quantitative distance measurements in systems such as membrane receptor stoichiometry,[40–43] protein folding,[44,45] protein conformational dynamics using temperature cycling[46] or orientation determination of biomolecules.[47] Moreover, the techniques can be used to obtain information on the position of light emission in multichromophore systems such as light-harvesting complexes or j-aggregates.[48,49]

Although we used localization in different blinking periods to decipher the signals of the two molecules, cryogenic localization microscopy can also be carried out in the context of stochastic photo-activation.[14,50,51] In fact, cryogenic photoswitching of fluorescent proteins has been reported in the literature about a decade ago,[52] and the required techniques for the preparation of biological samples have been developed in the field of cryogenic electron microscopy. All these strategies would benefit from yet higher precision and accuracy than demonstrated here. One possible way to increase the localization precision is to use a microscope objective with higher NA. In addition to a smaller PSF size, this will result in an increased collection efficiency and number of detected photons. For example, the use of a solid immersion lens with a refractive index of $n = 2.2$ would increase the number of detected photons by a factor of five and would reduce the size of the PSF by a factor of three, resulting in about $3\sqrt{5} \approx 7$ times higher localization precision. As discussed above, in this case one would have to consider the systematic errors that arise from the orientation of the dipole emitters close to an interface. Another issue that has to be considered for colocalization of molecules spaced at very small distances is the effect of dipole-dipole coupling.[10] We are currently investigating this and related phenomena.

Experimental Section

Sample Fabrication

A DNA strand with the sequence GCGAGTTCCACCTACCCTGCCTAAGCCTGTATC(C6dT)GTCA was labeled at position 34, where C6dT represents the modified thymidine deoxynucleotide with a flexible linker containing six methylene groups and a terminal amine group. This strand was annealed to different labeled oli-

© 2014 Wiley-VCH Verlag GmbH & Co. KGaA, Weinheim

gonucleotides with each construct resulting in a different sequence separation. The sequence of the complementary second strand was CGCTCAAGGTGGATGGGACGGATTCGGACATAGACAGT with the nucleotide at either position 4, 14, 20, or 24 replaced by C6dT. The first strand additionally contained a biotinylated poly-A tail for surface immobilization for room-temperature experiments that were not discussed here. Modified oligonucleotides were purchased from Microsynth AG (Balgach, Switzerland), purified with ion-exchange chromatography and labeled with Alexa Fluor 532 succinimidyl ester (Invitrogen). The two strands were then hybridized to obtain a double-stranded DNA. Since double-stranded DNA has a persistence length of about 50 nm, we expect our short DNA constructs (less than 15 nm long) to behave like rigid rods.[53]

The samples for microscopy were prepared by spin coating (10 s at 1000 rpm followed by 30 s at 3000 rpm) the labeled DNA constructs. A buffer solution with 130 μL Tris-EDTA buffer [Fluka, BioUltra (10 mM Tris-HCl; 1 mM EDTA; pH 7.4)] was prepared with 5 μL of 1 M $MgCl_2$ [Sigma (anhydrous, $\geq$98%)]. Next, 10 μL of a diluted solution of about 0.5 μM of the DNA constructs was added. 3 μL of this stock solution was then spin coated on fused silica cover slips (thickness 170 μm, Esco Products) that were cut to about 7×7 mm^2 square pieces before they were thoroughly cleaned by alternating oxygen plasma and rinsing with deionized water as well as non-halogenated solvents (acetone, ethanol, methanol, and 2-propanol, in that order). The samples were placed in the cryostat chamber immediately after preparation.

Cryogenic and Optical Setup

Technical details of the experimental setup and the localization fitting procedure can be found in ref. [21]. In short, the experiments were performed on a homebuilt epi-fluorescence microscope, numerical aperture 0.75, with the sample being mounted in a liquid helium flow cryostat. We minimized mechanical vibrations and drifts by a rigid and centrosymmetric setup design, and waiting for the setup to be settled after the initial cooling down and every mechanical movement. Furthermore, we accounted for a remaining long-term drift on the order of 100 nm per hour by tracking fiduciary markers.

Acknowledgements

This work was supported by the Max Planck Society and an Alexander-von-Humboldt Professorship. Ben Schuler acknowledges funding from the Swiss National Science Foundation and the European Research Council.

Keywords: angstrom accuracy · fluorescence · nanoscopy · single-molecule studies · super-resolution

[1] S. W. Hell, *Nat. Methods* **2009**, *6*, 24.
[2] Method of the year 2008 (Editorial) *Nat. Methods* **2009**, *6*, 1.
[3] W. K. Heisenberg, *The Physical Principles of the Quantum Theory*, Chicago University Press, Chicago, **1930**.
[4] J. Gelles, B. J. Schnapp, M. P. Sheetz, *Nature* **1988**, *331*, 450.
[5] E. Betzig, *Opt. Lett.* **1995**, *20*, 237.
[6] F. Güttler, T. Irngartinger, T. Plakhotnik, A. Renn, U. P. Wild, *Chem. Phys. Lett.* **1994**, *217*, 393.
[7] A. M. Van Oijen, J. Köhler, J. Schmidt, M. Müller, G. J. Brakenhoff, *J. Opt. Soc. Am. A* **1999**, *16*, 909.
[8] W. E. Moerner, L. Kador, *Phys. Rev. Lett.* **1989**, *62*, 2535.
[9] M. Orrit, J. Bernard, *Phys. Rev. Lett.* **1990**, *65*, 2716.
[10] C. Hettich, C. Schmitt, J. Zitzmann, S. Kühn, I. Gerhardt, V. Sandoghdar, *Science* **2002**, *298*, 385.
[11] T. D. Lacoste, X. Michalet, F. Pinaud, D.S. Chemla, A. P. Alivisatos, S. Weiss, *Proc. Natl. Acad. Sci. USA* **2000**, *97*, 9461.
[12] A. Pertsinidis, Y. Zhang, S. Chu, *Nature* **2010**, *466*, 647.
[13] E. Betzig, G. H. Patterson, R. Sougrat, O. W. Lindwasser, S. Olenych, J. S. Bonifacino, M. W. Davidson, J. Lippincott-Schwartz, H. F. Hess, *Science* **2006**, *313*, 1642.
[14] M. J. Rust, M. Bates, X. Zhuang, *Nat. Methods* **2006**, *3*, 793.
[15] S. T. Hess, T. P. K. Girirajan, M. D. Mason, *Philos. Mag.* **2006**, *91*, 4258.
[16] K. I. Mortensen, L. S. Churchman, J. A. Spudich, H. Flyvbjerg, *Nat. Methods* **2010**, *7*, 377.
[17] S. A. McKinney, C. S. Murphy, K. L. Hazelwood, M. W. Davidson, L. L. Looger, *Nat. Methods* **2009**, *6*, 131.
[18] A. Yildiz, J. N. Forkey, S. A. McKinney, T. Ha, Y. E. Goldman, P. R. Selvin, *Science* **2003**, *300*, 2061.
[19] J. C. Vaughan, S. Jia, X. Zhuang, *Nat. Methods* **2012**, *9*, 1181.
[20] S. F. Lee, Q. Vérolet, A. Fürstenberg, *Angew. Chem.* **2013**, *125*, 9117; *Angew. Chem. Int. Ed.* **2013**, *52*, 8948.
[21] S. Weisenburger, B. Jing, A. Renn, V. Sandoghdar, *Proc. SPIE* 8815:88150D-88150D-9, **2013**.
[22] M. P. Gordon, T. Ha, P. R. Selvin, *Proc. Natl. Acad. Sci. USA* **2004**, *101*, 6462.
[23] X. Qu, D. Wu, L. Mets, N. F. Scherer, *Proc. Natl. Acad. Sci. USA* **2004**, *101*, 11298.
[24] D. T. Burnette, P. Sengupta, Y. Dai, J. Lippincott-Schwartz, B. Kachar, *Proc. Natl. Acad. Sci. USA* **2011**, *108*, 21081.
[25] P. D. Simonson, E. Rothenberg, P. R. Selvin, *Nano Lett.* **2011**, *11*, 5090.
[26] Sparse bayesian step-filtering for high-throughput analysis of molecular machine dynamics. M. A. Little, N. S. Jones in *IEEE International Conference on Acoustics, Speech and Signal Processing*, **2010**, p. 4162.
[27] S. O. Rice, *Bell Syst. Tech. J.* **1945**, *24*, 46.
[28] F. Cichos, C. von Borczyskowski, M. Orrit, *Curr. Opin. Colloid Interface Sci.* **2007**, *12*, 272.
[29] R. Luchowski, E. G. Matveeva, I. Gryczynski, E. A. Terpetschnig, L. Patsenker, G. Laczko, J. Borejdo, Z. Gryczynski, *Curr. Pharm. Biotechnol.* **2008**, *9*, 411.
[30] M. Lippitz, C. G. Hübner, T. Christ, H. Eichner, P. Bordat, A. Herrmann, K. Müllen, T. Basché, *Phys. Rev. Lett.* **2004**, *92*, 103001.
[31] R. Métivier, F. Nolde, K. Müllen, T. Basché, *Phys. Rev. Lett.* **2007**, *98*, 047802.
[32] R. E. Thompson, D. R. Larson, W. W. Webb, *Biophys. J.* **2002**, *82*, 2775.
[33] R. J. Ober, S. Ram, E. S. Ward, *Biophys. J.* **2004**, *86*, 1185.
[34] J. Jung, S. Weisenburger, S. Albert, D. F. Gilbert, O. Friedrich, V. Eulenburg, J. Kornhuber, T. W. Groemer, *Microsc. Res. Tech.* **2013**, *76*, 835.
[35] A. P. Bartko, R. M. Dickson, *J. Phys. Chem. B* **1999**, *103*, 11237.
[36] J. Enderlein, E. Toprak, P. R. Selvin, *Opt. Express* **2006**, *14*, 8111.
[37] J. Engelhardt, J. Keller, P. Hoyer, M. Reuss, T. Staudt, S. W. Hell, *Nano Lett.* **2011**, *11*, 209.
[38] M. D. Lew, M. P. Backlund, W. E. Moerner, *Nano Lett.* **2013**, *13*, 3967.
[39] A. Agrawal, S. Quirin, G. Grover, R. Piestun, *Opt. Express* **2012**, *20*, 26667.
[40] P. Hastie, M. H. Ulbrich, H. Wang, R. J. Arant, A. G. Lau, Z. Zhang, E. Y. Isacoff, L. Chen, *Proc. Natl. Acad. Sci. USA* **2013**, *110*, 5163.
[41] D. Calebiro, F. Rieken, J. Wagner, T. Sungkaworn, U. Zabel, A. Borzi, E. Cocucci, A. Zürn, M. J. Lohse, *Proc. Natl. Acad. Sci. USA* **2013**, *110*, 743.
[42] A. Pertsinidis, K. Mukherjee, M. Sharma, Z. P. Pang, S. R. Park, Y. Zhang, A. T. Brunger, T. C. Sdhof, S. Chu, *Proc. Natl. Acad. Sci. USA* **2013**, *110*, E2812–E2820.
[43] M. Scarselli, P. Annibale, C. Gerace, A. Radenovic, *Biochem. Soc. Trans.* **2013**, *41*, 191.
[44] A. Borgia, P. M. Williams, J. Clarke, *Annu. Rev. Biochem.* **2008**, *77*, 101.
[45] B. Schuler, H. Hofmann, *Curr. Opin. Struct. Biol.* **2013**, *23*, 36.
[46] H. Yuan, T. Xia, B. Schuler, M. Orrit, *Phys. Chem. Chem. Phys.* **2011**, *13*, 1762.

© 2014 Wiley-VCH Verlag GmbH & Co. KGaA, Weinheim

[47] P. Kukura, H. Ewers, C. Müller, A. Renn, A. Helenius, V. Sandoghdar, *Nat. Methods* **2009**, *6*, 923.
[48] D. L. Andrews, C. Curutchet, G. D. Scholes, *Laser Photonics Rev.* **2011**, *123*, 114.
[49] F. Würthner, T. E. Kaiser, C. R. Saha-Möller, *Angew. Chem.* **2011**, *123*, 3436; *Angew. Chem. Int. Ed.* **2011**, *50*, 3376.
[50] M. Heilemann, E. Margeat, R. Kasper, M. Sauer, P. Tinnefeld, *J. Am. Chem. Soc.* **2005**, *127*, 3801.
[51] A. R. Faro, P. Carpentier, G. Jonasson, G. Pompidor, D. Arcizet, I. Demachy, D. Bourgeois, *J. Am. Chem. Soc.* **2011**, *133*, 16362.
[52] T. M. H. Creemers, A. J. Lock, V. Subramaniam, T. M. Jovin, S. Völker, *Proc. Natl. Acad. Sci. USA* **2000**, *97*, 2974.
[53] P. J. Hagerman, *Annu. Rev. Biophys. Biophys. Chem.* **1988**, *17*, 265.

Received: November 17, 2013
Revised: January 18, 2014
Published online on February 20, 2014

© 2014 Wiley-VCH Verlag GmbH & Co. KGaA, Weinheim